

The origin of the slow solar wind in coronal streamers

L. Ofman^{a,*}

^a *The Catholic University of America, NASA Goddard Space Flight Center, Mail Code 682, Greenbelt, MD 20771, USA*

Abstract

The highly variable slow solar wind has been associated with low-latitude regions of the heliosphere most clearly by the Ulysses spacecraft. Although, it is evident today that the slow solar wind originates in coronal helmet streamers, the mechanism of the slow solar wind acceleration, and the origin of the variability are still being debated. The combination of new observations and numerical modeling are beginning to address these questions. I will discuss how recent in-situ observations by Ulysses, white light and EUV observations by the LASCO and UVCS instruments on SOHO advanced our understanding of the streamer structure, dynamics, and stability. I will briefly review the current state of numerical MHD modeling of streamers, and the possible mechanisms that may produce the highly variable slow wind. I will present the results of recent heat-conductive MHD modeling of multiple streamer slow solar wind with heating function constrained by observations. I will show how multi-fluid numerical modeling of the slow solar wind in streamers helps to identify the regions of the slow solar wind outflow.

© 2003 COSPAR. Published by Elsevier Ltd. All rights reserved.

Keywords: Sun; Corona; Solar wind; MHD; Multi-fluid equations; Satellite observations

1. Introduction

The Ulysses spacecraft (McComas et al., 2000), ACE (Stone et al., 1998), and WIND (Acuña et al., 1995) satellites, the SOHO UVCS (Raymond et al., 1997; Habbal et al., 1997; Li et al., 1998; Strachan et al., 2002), LASCO (Sheeley et al., 1997; Tappin et al., 1999; Lewis and Simnett, 2002), and Doppler Scintillation measurements (e.g., Woo and Gazis, 1994) are a partial list of observations that provide detailed information on the composition, outflow velocities, the distribution function with its moments (density, temperature, etc.), magnetic field far from the Sun (Ulysses, ACE), and outflow velocities, densities, and temperatures close to the sun (UVCS, LASCO). The observations associate the slow solar wind with the high-density equatorial streamer belt regions. However, in spite of the wealth of observational data the exact physical mechanism responsible for the heating and the acceleration of the slow solar wind is poorly understood at present. In part this is due to the fact that most of the detailed observations of the solar wind were obtained far from the Sun, while there are no sufficiently detailed observations

in the acceleration region close to the Sun, and in part due to the lack of sufficiently detailed physics in current models.

The main approach that may improve the understanding of the slow solar wind formation is to supplement the observations with kinetic and MHD numerical modeling. Kinetic modeling of the slow wind is difficult since it requires the solution of the time-dependent Boltzmann's equation in six dimensions, with poorly known boundary conditions, evolution of the collision term from collisional to nearly collisionless regime, and forces. To model the acceleration of the solar wind in coronal streamers using MHD equations at least two spatial dimensions are required. Pneuman and Kopp (1971) in their classic work attempted the first 2D MHD steady state model of a self-consistent solar wind flow in a coronal streamer. Their model was isothermal and required iterations between the 2D magnetic field solutions and 1D solar wind flow solutions along the field lines. For the past three decades the coronal streamers were extensively modeled with steady state 2D MHD models (Steinolfson et al., 1982; Washimi et al., 1987; Cuperman et al., 1990, 1995; Usmanov, 1993a; Wang et al., 1993; Suess et al., 1994, 1996; Bravo and Stewart, 1997; Stewart and Bravo, 1997; Wiegmann et al., 2000), as part of 3D MHD global models (Linker et al.,

* Tel.: +1-301-286-9913; fax: +1-301-286-1617.

E-mail address: ofman@waves.gsfc.nasa.gov (L. Ofman).

1990; Usmanov, 1993b; Pizzo, 1995; Mikić and Linker, 1996; Mikić et al., 1999). Realizing that the heat input and losses are significantly different between protons, electrons, and minor ions two-fluid models (Suess et al., 1999), and three-fluid models of the slow solar wind in streamers were recently developed (Ofman, 2000). Usually, in the above models an isothermal, or polytropic energy equation was solved, or an ad-hoc heating function was introduced.

Recently, semi-empirical modeling of coronal streamers that combines observational constraints with MHD solution was proposed by Sittler and Guhathakurta (1999). With this approach observational constraints are used to quantify the momentum and the heat input in the solar wind (Sittler et al., 2003). In this model the observed magnetic field at 1 AU and on the sun are used as boundary conditions for the MHD equations.

An alternative view of the formation of the slow solar wind in the magnetized wake of a streamer was considered by several authors (Dahlburg et al., 1998; Einaudi et al., 1999, 2001). In this model the slow solar wind is produced by the combination of tearing mode and Kelvin–Helmholtz instabilities in the velocity and magnetic field shear layers believed to exist in the streamer wakes. Another alternative view suggests that reconnection of coronal loops with overlaying open magnetic field lines is responsible for the slow solar wind formation (Fisk et al., 1998). This view is motivated by the minor ion compositional differences (i.e., FIP effect) between the slow and fast solar wind observed by ACE and Ulysses.

The main unresolved questions on the properties and the formation of the slow solar wind are the following:

- What is the physical mechanism that produces the unsteady slow solar wind?
- What is the role of reconnection and waves in producing the slow wind?
- What role does the streamer magnetic, density, and temperature structure play in the heating and the acceleration of the slow solar wind?
- What are the stability properties of streamers?
- What leads to the compositional differences between the fast and slow solar wind plasma?
- What heats the slow solar wind electrons and ions?

Several recent observations and modeling efforts that are aimed at addressing these questions will be discussed below.

2. Observations of slow solar wind

Perhaps the most striking observations of the slow solar wind are the Ulysses observations that exemplify the difference between the slow and fast wind as the spacecraft travels out of the ecliptic plane. In addition

ACE and WIND satellites provide detailed information of the slow solar wind velocity, composition, density, energy, and magnetic field near 1 AU. The SOHO LASCO white light observations that use the motion of small density enhancements, or “blobs” in the slow solar wind to trace the slow solar wind speed.

The unsteady nature of the slow solar wind far from the Sun is most evident in Ulysses/SWOOPS ion detector measurements of the solar wind outflow velocity and density near the ecliptic plane. In Fig. 1 McComas et al. (2000) show the latitudinal dependence of the velocity and density scaled to 1 AU near minimum of solar activity cycle. According to McComas et al. (2000) variability of the low-latitude solar wind in the Ulysses measurements is likely due to the inclination of the equatorial streamer belt relative to the solar equator, which results in “overlapping” regions of fast solar wind emerging from coronal holes with the slow wind from streamers. It is thought that the interaction between the fast and slow solar wind in corotating interacting regions (CIRs) contributes to the solar wind variability.

The most direct observation of the slow solar wind in the inner corona was first obtained by Sheeley et al. (1997) using the SOHO LASCO instrument (see also Lewis and Simnett, 2002). Sheeley et al. (1997) investigated the outflow motions of small density enhancements emerging from streamers as proxies to the slow

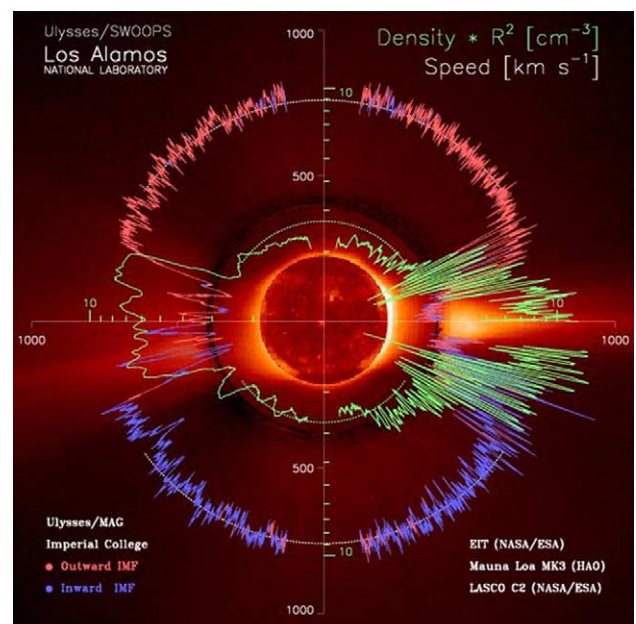


Fig. 1. Ulysses observations of the solar wind in the ecliptic plane and over the poles. The gray (red and blue in the color online version of this figure) lines in the polar plot show the solar wind speed for outward and inward magnetic field direction. The white (green in the color online version of this figure) line shows the density on the logarithmic scale. For reference, the polar plot is overlaid with the SOHO LASCO/C2 and Mauna Loa MK3 Coronagraph images, and with the SOHO EIT image of the solar disk (adapted from McComas et al., 2000).

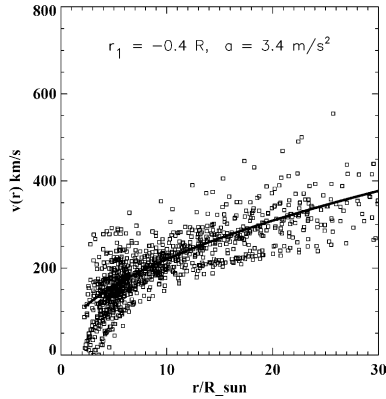


Fig. 2. The outflow velocity of 65 density enhancements emerging from streamers analyzed by Sheeley et al. (1997). The solid line is the best fit of $v^2 = 2a(r - r_1)$. The moving density enhancements (blobs) are believed to trace the slow solar wind speed (adapted from Sheeley et al., 1997).

solar wind flow. In Fig. 2 the outflow velocity of 65 density enhancements emerging from streamers analyzed by Sheeley et al. (1997) are shown. The solid line is the best fit of $v^2 = 2a(r - r_1)$. The moving density “blobs” are believed to trace the slow solar wind speed, and the spread is of the order of 100 km s^{-1} . This spread is likely due to the combined variation of the properties of the streamers (e.g., temperature, density, heat input), and the properties of the blobs.

The SOHO UVCS provides spectroscopic information on the slow solar wind in the inner corona (Raymond et al., 1997; Strachan et al., 2002) (see Figs. 6 and 7). For example, recently Strachan et al. (2002) determined the oxygen ion outflow velocities as a function of height and latitude in an equatorial streamer. They found that the outflow velocity increases abruptly from the core of the streamer to the streamer legs, with no flows in the core within the error bars. This suggests that the slow solar wind outflow is along the open field lines that surround the streamer core (streamer “legs”). These observations provide constraints for three fluid models of the slow solar wind (Ofman, 2000).

3. Slow solar wind models

Below I will summarize several common approaches that are used to model solar coronal streamers and the slow solar wind.

3.1. Polytropic MHD model

The polytropic MHD model is based on a simplified form of the energy equations, with the polytropic index $\gamma = 1$ for an isothermal model, or 1.05 for nearly isothermal polytropic flow. The normalized MHD equations with standard notation for the variables (e.g., Usmanov, 1993b; Ofman and Davila, 1998) are

$$\frac{\partial \rho}{\partial t} + \nabla \cdot (\rho \mathbf{v}) = 0, \quad (1)$$

$$\frac{\partial \mathbf{v}}{\partial t} + (\mathbf{v} \cdot \nabla) \mathbf{v} = -\frac{Eu}{\rho} \nabla p - \frac{1}{Fr r^2} + \frac{\mathbf{J} \times \mathbf{B}}{\rho}, \quad (2)$$

$$\frac{\partial \mathbf{B}}{\partial t} = \nabla \times (\mathbf{v} \times \mathbf{B}) + S^{-1} \nabla^2 \mathbf{B}, \quad (3)$$

$$\left(\frac{\partial}{\partial t} + \mathbf{v} \cdot \nabla \right) \frac{p}{\rho^\gamma} = 0. \quad (4)$$

In the above equations the normalization is $r \rightarrow r/R_\odot$, $t \rightarrow t/\tau_A$, $v \rightarrow v/v_A$, $B \rightarrow B/B_0$, $\rho \rightarrow \rho/\rho_0$, and $p \rightarrow p/p_0$, where, R_\odot is the solar radius, $\tau_A = R_\odot/v_A$ is the Alfvén time, $v_A = B_0/\sqrt{4\pi\rho_0}$ is the Alfvén velocity, B_0 is the magnetic field, ρ_0 is the density, and p_0 is the pressure. Other physical parameters are the Lundquist number S , the Froude number $Fr = v_A^2 R_\odot/(GM_\odot)$, where G is the gravitational constant and M_\odot is the solar mass, and the Euler number $Eu = p_0/(\rho_0 v_A^2) = c_s^2/\gamma v_A^2$, where c_s is the speed of sound.

The polytropic model produces qualitatively correct slow solar wind solutions in streamers. In Fig. 3 a typical polytropic solution obtained with the 2.5D MHD model of the inner solar corona with three streamers is shown. The left panel shows the temperature in units of 1.6 MK, the middle panel shows the Ohmic heating power per unit mass and per unit resistivity (j^2/ρ) in units of $10^{14} \text{ erg}/(\text{s}^2 \text{ g})$, and the right panel shows the slow solar wind velocity vectors with the maximal solar wind speed of 165 km s^{-1} . In this model the magnetic field strength at the bases of the corona is 12 G.

The magnetic field and density boundary conditions are based on observational values (see, Sittler and Guhathakurta, 1999). The polytropic model was applied successfully to model the three dimensional inner solar corona by Mikić et al. (1999), using the magnetic field data from NSOKP and WSO as the boundary conditions. In Fig. 4 the results of the 3D MHD calculations are compared to eclipse observations.

Although the density values of the streamers generally do not agree with the observed density, it is evident that this model provides good qualitative agreement between the calculated and the observed streamer structures from which the slow solar wind originates.

3.2. Thermally conductive MHD model

The polytropic model provides only qualitative slow solar wind velocity and density structure, with rudimentary temperature structure. For example, the polytropic model produces constant (for $\gamma = 1$) or radially decreasing (for $\gamma = 1.05$) temperature profile. However, observations show that the average coronal temperature peaks at $r > 1R_\odot$ (e.g., $r \sim 1.5R_\odot$ in Sittler and

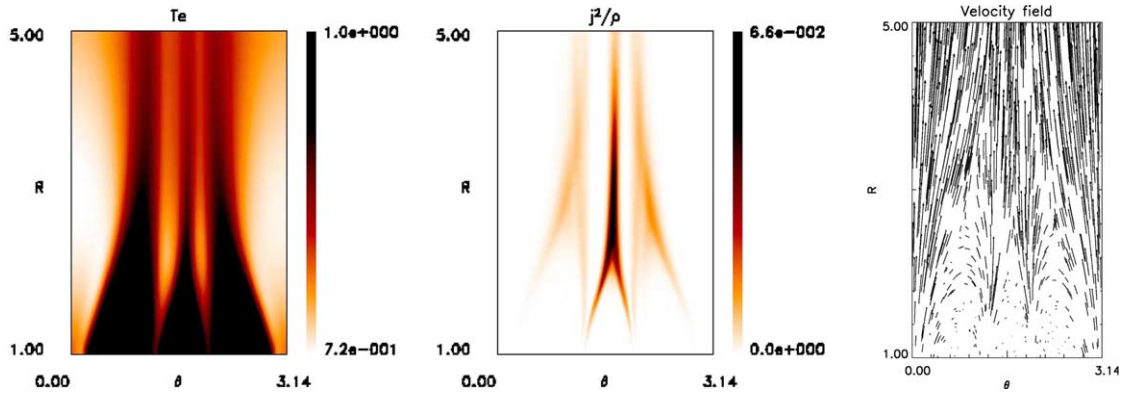


Fig. 3. The polytropic 2.5D coronal model with three streamers. The left panel shows the temperature in units of 1.6 MK, the middle panel shows the Ohmic heating density (j^2/ρ) in arbitrary units, and the right panel shows the slow solar wind velocity vectors with the maximal speed of 165 km s^{-1} .

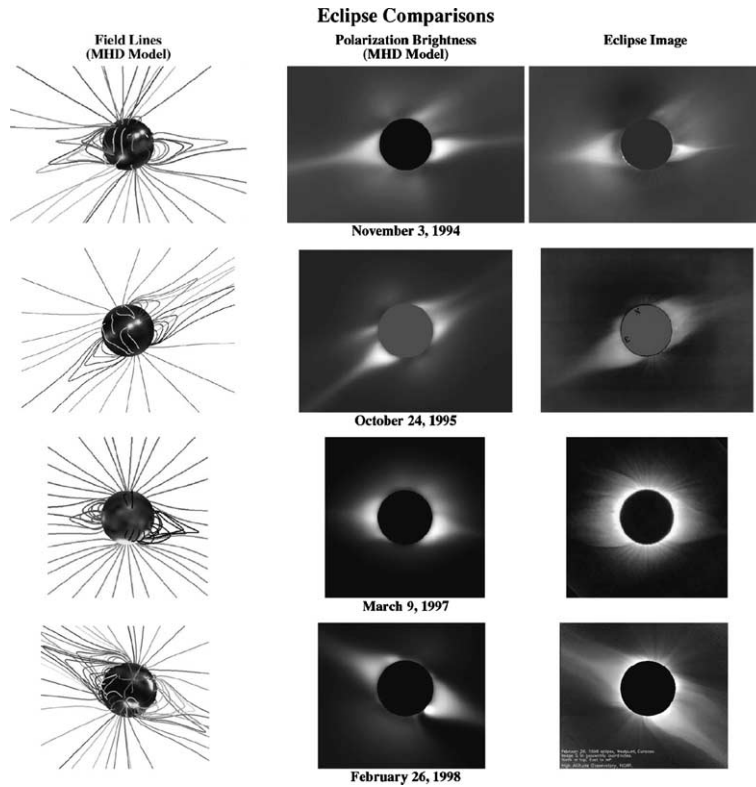


Fig. 4. Comparison of polytropic 3D MHD computations of the solar corona using magnetic field data from NSOKP and WSO with total solar eclipse observations. With this model a good qualitative agreement between the modeled and the observed streamer structure is achieved (adapted from Mikić et al., 1999).

Guhathakurta, 1999). The heat conductive model can produce a temperature profile that is more consistent with observations. The observed average mass flux of the solar wind can be better matched with heat conductive models. Thus, to improve the slow solar wind modeling one needs to use the thermally conductive energy equation instead of Eq. (4) in the MHD equations. In terms of temperature the energy equations can be written as

$$\frac{\partial T}{\partial t} = -(\gamma - 1)T\nabla \cdot \mathbf{V} - \mathbf{V} \cdot \nabla T + (\gamma - 1)(H_c/\rho + H_i), \tag{5}$$

where $\gamma = 5/3$, $H_c = \nabla(\xi T^{5/2} \frac{\nabla T \cdot \mathbf{B}}{B^2}) \cdot \mathbf{B}$ is the heat conduction term projected on the magnetic field lines, ξ is the thermal conductivity coefficient, and H_i is the heating term. The heating term can be parameterized with an expression of the form $H_i = H_0(r - 1)e^{-r/2}$, where the

values of H_0 , and λ are chosen to match the observed solar wind temperature and mass flux at observed locations. In addition, to match the fast solar wind speed in coronal holes an ad-hoc momentum input term P_i can be added to the r.h.s. of Eq. (2) (e.g. Suess et al., 1996).

In Fig. 5 typical slow solar wind solutions obtained with the thermally conductive MHD model are shown. The initial magnetic field was a multipolar expansion that qualitatively matches observations. After the model was evolved for about 11 h to a steady state, coronal streamers with open field lines and slow solar wind outflow reaching 157 km s^{-1} at $5R_\odot$ have formed. The upper left panel shows the magnetic field vectors, the upper right panel shows the outflow velocity vectors of the solar wind, the lower left panel shows the temperature structure, and the lower right panel shows the ohmic heating term due to the current “sheets” of the streamers. The effect of heat input and thermal conduction is most evident in the temperature structure in Fig. 5 compared to Fig. 3.

3.3. Semi-empirical MHD model

Recently, Sittler and Guhathakurta (1999) have proposed a semi-empirical approach to model the formation of both, fast and slow solar wind. With this approach the heat and the momentum input into the solar wind are estimated based on quantitative obser-

vational constrains. The present version of this approach is outlined as follows:

1. The magnetic field and the solar wind are calculated using MHD model with photospheric boundary conditions, and a zero-order heat and momentum input.
2. The effective heat flux and effective temperature are estimated empirically by solving energy and momentum conservation equations along open field lines using measured solar wind parameters at 1 AU, and the magnetic field from #1.
3. The magnetic field configuration and the solar wind are recalculated using MHD model with updated heat flux and effective temperature.

Early results with this approach show that the formations of the slow solar wind can be understood in terms of heat input alone, in contrast to the fast solar wind, which requires momentum input in addition to heat input (Sittler et al., 2003).

3.4. Multi-fluid model

Observations show that the electrons, protons, and various minor ions in the solar corona and the solar wind have dramatically different thermodynamic properties and outflow speeds. In addition there are compositional differences between the fast and slow solar wind. Thus, understanding the dynamics and kinetics of minor ions is crucial for the interpretation of these ob-

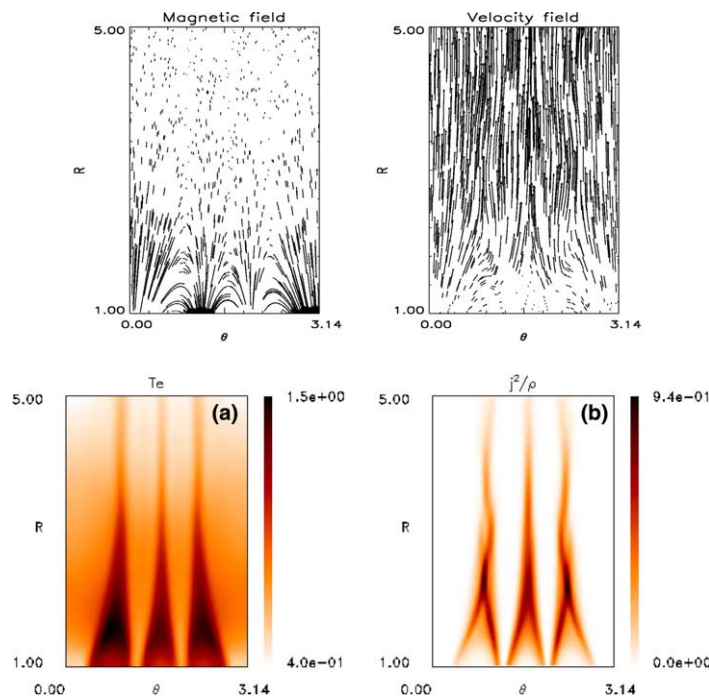


Fig. 5. Results of thermally conductive three-streamer coronal model. The upper left panel shows the magnetic field vectors, the upper right panel shows the outflow velocity vectors of the solar wind, the lower left panel (a) shows the temperature structure, and the lower right panel (b) shows the ohmic heating due to the current “sheets” of the streamers (adapted from Sittler et al., 2003).

servations. In the weakly collisional coronal plasma the normalized three-fluid MHD equations are (see Ofman, 2000)

$$\frac{\partial n_k}{\partial t} + \nabla \cdot (n_k \mathbf{V}_k) = 0,$$

$$n_k \left[\frac{\partial \mathbf{V}_k}{\partial t} + (\mathbf{V}_k \cdot \nabla) \mathbf{V}_k \right] = -Eu_k \nabla p_k - Eu_e \frac{Z_k n_k}{A_k n_e} \nabla p_e, \quad (6)$$

$$-\frac{n_k}{Fr r^2} + \frac{Z_k n_k}{A_k n_e} (\nabla \times \mathbf{B}) \times \mathbf{B} + F_{k,\text{coul}}, \quad (7)$$

$$\frac{\partial \mathbf{B}}{\partial t} = -\nabla \times \mathbf{E}, \quad \mathbf{E} = -\mathbf{V}_e \times \mathbf{B} + \frac{1}{S} \nabla \times \mathbf{B}, \quad (8)$$

$$\mathbf{V}_e = \frac{1}{n_e} (n_p \mathbf{V}_p + Z n_i \mathbf{V}_i - b \nabla \times \mathbf{B}), \quad (9)$$

$$\frac{\partial T_k}{\partial t} = -(\gamma_k - 1) T_k \nabla \cdot \mathbf{V}_k - \mathbf{V}_k \cdot \nabla T_k, \quad (10)$$

where the index $k = p, i$ (in Eq. (10) $k = e, p, i$) and p is protons, i is ions, and e is electrons. The following normalization is used: $r \rightarrow r/R_\odot$, where R_\odot is the solar radius; $t \rightarrow t/\tau_A$; $V \rightarrow V/V_A$; $B \rightarrow B/B_0$; $n_{i,e,p} \rightarrow n_{i,e,p}/n_{e0}$; $S = \tau_r/\tau_A$ the Lundquist number; $\tau_r = 4\pi R_\odot^2/\nu c^2$ the resistive time scale, where ν is the resistivity, and c is the speed of light; $\tau_A = R_\odot/V_A$ the Alfvén time scale; $V_A = B_0/(4\pi m_p n_e)^{1/2}$ is the Alfvén speed; $Eu_{e,p} = (k_b T_{e,p,0}/m_p)/V_A^2$ the electron or proton Euler number; $Eu_i = (k_b T_{i,0}/m_i)/V_A^2$ the ion Euler number; $Fr = V_A^2 R_\odot/(GM_\odot)$ the Froude number, where G is the universal gravitational constant and M_\odot is the solar mass; and the normalization constant; $b = cB_0/(4\pi e n_{e0} R_\odot V_A)$, where A_k is the atomic mass of each species, and Z_k is the charge state. The Coulomb friction term $F_{k,\text{coul}}$ is given in Ofman and Davila (2001). In this model Ofman (2000) assumed that the corona is nearly isothermal (i.e.,

$\gamma_k \approx 1$), did not include heat sources explicitly, and assumed flows parallel to magnetic field lines in the momentum equations. The polytropic indices in this model are $\gamma_{O^{5+}} = 1$, and $\gamma_p = \gamma_e = 1.05$.

Results of the three-fluid model are compared to SOHO/UVCS observations in Figs. 6 and 7. The model was initiated with a dipole magnetic field and a uniform proton and ion density. The model was run until the streamer was formed self-consistently and reached a steady state after about 16 h. The current “sheet” has a resolved finite thickness determined by the resistivity and Hall terms in the code (the Lundquist number was 10^5). The qualitative agreement between the model calculations of the proton and ion density structure, and the UVCS observations is evident in Fig. 6. Ofman (2000) found that due to Coulomb friction the oxygen ions flow with the protons in the open field line regions, and thus mark the outflow of the slow solar wind in the spectroscopic observations.

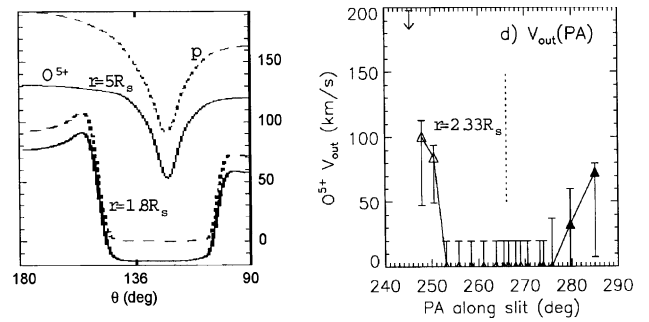


Fig. 7. Proton and oxygen ion outflow velocities across the streamer. Three fluid results of a model streamer are shown in the left panel (based on Ofman, 2000); UVCS observations of the oxygen ions outflow velocity across a streamer observed during April 23–27, 1997 are shown on the right panel (adapted from Strachan et al., 2002).

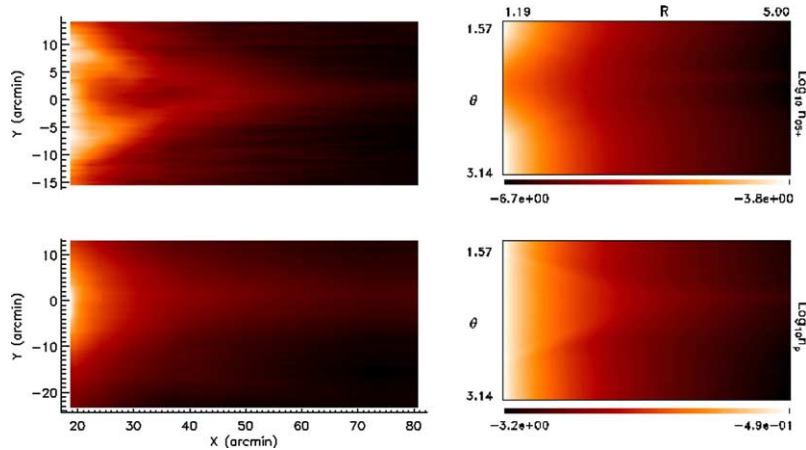


Fig. 6. Comparison of SOHO/UVCS 12 October 1996 observation of an equatorial streamer in O VI (upper left panel) and in Ly α (lower left panel) with the results of the three-fluid model of a coronal streamer. In the model, the density is given in units of 10^8 cm^{-3} , and θ is in radians. Note the good qualitative agreement between observations and model of the oxygen ion bifurcated streamer structure (the two left panels were adapted from Kohl et al., 1997; the two right panels were adapted from Ofman, 2000).

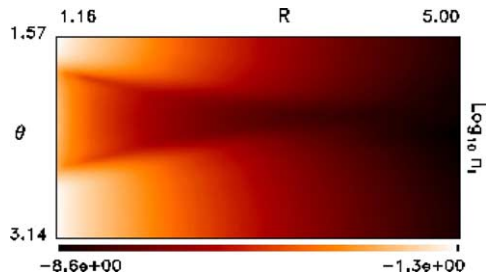


Fig. 8. Same as upper right panel in Fig. 6, but for He^{++} ions.

In Fig. 7 a cut across the latitudinal direction of a streamer observed during April 23–27, 1997 and analyzed by Strachan et al. (2002) is shown. For comparison, the latitudinal cut of the three-fluid streamer is also shown. The good qualitative agreement between model and observations of the outflow speed of O^{5+} ions is evident.

Future observations that will provide information on other minor ions, such as He^{++} , in the solar wind close to the sun will help to improve the multi-fluid modeling of the slow solar wind. The improved modeling will help to better understand the acceleration mechanism of the slow wind. The outflow of He^{++} ions in a streamer were modeled with the three fluid equations, by setting $A = 4$, $Z = 2$, with the temperature $T_{\text{He}} = 3$ MK, and density of 10% for helium ions. In Fig. 8 a typical result of this calculation is shown. It is evident that He^{++} streamer appears dark compared to the surrounding coronal plasma, similar to the effect seen in oxygen streamer. This is due to the Coulomb friction between the outflowing protons and He^{++} ions, and gravitational settling of He^{++} ions in the core of the streamer. The effect is stronger than in O^{5+} due to the higher collision frequency between electrons, protons and He^{++} ions, and due to the much higher density of He^{++} ions compared to O^{5+} ions.

4. Conclusions

In-situ and remote sensing observations show that the physical properties of the slow solar wind are strikingly different from the fast wind. The slow solar wind is not only slower by a factor of two than the fast wind, but also is much denser than the fast wind, and appears to be less steady. In addition the slow wind plasma has different minor ion composition, and temperature than the fast wind plasma. Coronal streamers have been identified as the source regions of the slow wind, with most direct evidence provided by the SOHO LASCO and UVCS instruments. Spectroscopic imaging observations by the SOHO UVCS of streamers in Ly α and OVI emission lines provide information about the source regions of the slow solar wind outflow of hydrogen and oxygen ions, and the relative abundance of the oxygen ions.

The slow solar wind in streamers has been modeled using 2D and 3D single fluid polytropic MHD as part of global models for decades. Models with more advanced energy equations, such as thermally conductive and semi-empirical models help to quantify the spatial distribution of the energy input required to produce the observed slow solar wind. The minor ion emission observations provide detailed information on the slow solar wind outflow regions, and require multi-fluid and kinetic modeling in order to interpret the results. In light of recent observations two- and three- fluid models of streamers were developed. These models can account for the different thermal properties of electrons, protons, and minor ions. Although the exact physical mechanism that produces the slow solar wind is unknown, recent models and observations strongly constrain the properties of this mechanism. Investigating the properties of streamers (B , T , n , n_{ion} , etc.) and their stability are also necessary for the understanding of the unsteady nature of the slow solar wind, and of coronal mass ejections (CMEs) associated with streamer eruptions. The role of high frequency waves, low frequency waves, reconnection, and turbulence needs to be explored self consistently in streamers in order to understand how the slow solar wind may be produced and affected by these processes.

Acknowledgements

This work was supported by NASA grants NAGS-11815, NAG5-11877, and NSF grant ATM-0135889.

References

- Acuña, M.H., Ogilvie, K.W., Baker, D.N., Curtis, S.A., Fairfield, D.H., Mish, W.H. The global geospace science program and its investigations. *Space Sci. Rev.* 71, 5–21, 1995.
- Bravo, S., Stewart, G.A. Fast and slow wind from solar coronal holes. *Astrophys. J.* 489, 992–999, 1997.
- Cuperman, S., Ofman, L., Dryer, M. Thermally conductive magnetohydrodynamic flows in helmet-streamer coronal structures. *Astrophys. J.* 350, 846–855, 1990.
- Cuperman, S., Bruma, C., Dryer, M., Semel, M. The magnetohydrodynamic equilibrium of coronal helmet streamers. *A&A* 299, 389–413, 1995.
- Dahlburg, R.B., Karpen, J.T., Einaudi, G., Bonicelli, P. Acceleration of the slow solar wind. *ESA SP-421: Solar Jets Coronal Plumes*, 199–206, 1998.
- Einaudi, G., Bonicelli, P., Dahlburg, R.B., Karpen, J.T. Formation of the slow solar wind in a coronal streamer. *J. Geophys. Res.* 104, 521–534, 1999.
- Einaudi, G., Chibbaro, S., Dahlburg, R.B., Velli, M. Plasmoid formation and acceleration in the solar streamer belt. *Astrophys. J.* 547, 1167–1177, 2001.
- Fisk, L.A., Schwadron, N.A., Zurbuchen, T.H. On the slow solar wind. *Space Sci. Rev.* 86, 51–60, 1998.

- Habbal, S.R., Woo, R., Fineschi, S., O'Neal, R., Kohl, J., Noci, G., Korendyke, C. Origins of the slow and the ubiquitous fast solar wind. *Astrophys. J. Lett.* 489, L103–L106, 1997.
- Kohl, J.L. et al. First results from the SOHO ultraviolet coronagraph spectrometer. *Solar Phys.* 175, 613–644, 1997.
- Lewis, D.J., Simnett, G.M. Bulk flow velocities in the solar corona at solar maximum. *MNRAS* 333, 969–976, 2002.
- Li, J., Raymond, J.C., Acton, L.W., Kohl, J.L., Romoli, M., Noci, G., Naletto, G. Physical structure of a coronal streamer in the closed-field region as observed from UVCS/SOHO and SXT/Yohkoh. *Astrophys. J.* 506, 431–438, 1998.
- Linker, J.A., van Hoven, G., Schnack, D.D. A three-dimensional simulation of a coronal streamer. *Geophys. Res. Lett.* 17, 2281–2284, 1990.
- McComas, D.J., Barraclough, B.L., Funsten, H.O., Gosling, J.T., Santiago-Muoz, E., Skoug, R.M., Goldstein, B.E., Neugebauer, M., Riley, P., Balogh, A. Solar wind observations over Ulysses' first full polar orbit. *J. Geophys. Res.* 105, 10419–10434, 2000.
- Mikić, Z., Linker, J.A. Large-scale structure of the solar corona and inner heliosphere, in: Winterhalter, D., et al. (Eds.), *Solar Wind Eight*, Conference Proc. 382, pp. 104–107, 1996.
- Mikić, Z., Linker, J.A., Schnack, D.D., Lionello, R., Tarditi, A. Magnetohydrodynamic modeling of the global solar corona. *Phys. Plasmas* 6, 2217–2224, 1999.
- Ofman, L. Source regions of the slow solar wind in coronal streamers. *Geophys. Res. Lett.* 27, 2885–2888, 2000.
- Ofman, L., Davila, J.M. Solar wind acceleration by large-amplitude nonlinear waves: parametric study. *J. Geophys. Res.* 103, 23677–23690, 1998.
- Ofman, L., Davila, J.M. Three-fluid 2.5-dimensional magnetohydrodynamic model of the effective temperature in coronal holes. *Astrophys. J.* 553, 935–940, 2001.
- Pizzo, V.J. Flow properties along field lines in a 3-D tilted-dipole geometry, *Solar Wind 8 Conference*, p. 43, 1995.
- Pneuman, G.W., Kopp, R.A. Gas-magnetic field interactions in the solar corona. *Solar Phys.* 18, 258–270, 1971.
- Raymond, J.C. et al. Composition of coronal streamers from the SOHO ultraviolet coronagraph spectrometer. *Solar Phys.* 175, 645–665, 1997.
- Sheeley, N.R. et al. Measurements of Flow Speeds in the Corona between 2 and 30 R_{sun} . *Astrophys. J.* 484, 472–478, 1997.
- Sittler, E.C., Guhathakurta, M. Semiempirical two-dimensional magnetohydrodynamic model of the solar corona and interplanetary medium. *Astrophys. J.* 523, 812–826, 1999.
- Sittler, E.C., Ofman, L., Gibson, S., Guhathakurta, M., Davila, J., Skoug, R., Fludra, A., Holzer, T. Development of Multidimensional MHD Model for the Solar Corona and Solar Wind, in: *Proceeding of the Solar Wind X*, Pisa, Italy, June 2002, AIP Conf. Proc. 679, 113–116, 2003.
- Steinolfson, R.S., Wu, S.T., Suess, S.T. The steady global corona. *Astrophys. J.* 255, 730–742, 1982.
- Stewart, G.A., Bravo, S. Latitudinal solar wind velocity variations from polar coronal holes: a self-consistent MHD model. *J. Geophys. Res.* 102, 11263–11272, 1997.
- Suess, S.T., Wu, S.T., Wang, A.-H., Poletto, G. Magnetohydrodynamic simulation of a streamer beside a realistic coronal hole. *Space Sci. Rev.* 70, 295–298, 1994.
- Suess, S.T., Wang, A.-H., Wu, S.T. Volumetric heating in coronal streamers. *J. Geophys. Res.* 101, 19957–19966, 1996.
- Suess, S.T., Wang, A.-H., Wu, S.T., Poletto, G., McComas, D.J. A two-fluid, MHD coronal model. *J. Geophys. Res.* 104, 4697–4708, 1999.
- Stone, E.C., Frandsen, A.M., Mewaldt, R.A., Christian, E.R., Margolies, D., Ormes, J.F., Snow, F. The advanced composition explorer. *Space Sci. Rev.* 86, 1–22, 1998.
- Strachan, L., Suleiman, R., Panasyuk, A.V., Biesecker, D.A., Kohl, J.L. Empirical densities, kinetic temperatures, and outflow velocities in the equatorial streamer belt at solar minimum. *Astrophys. J.* 571, 1008–1014, 2002.
- Tappin, S.J., Simnett, G.M., Lyons, M.A. A determination of the outflow speeds in the lower solar wind. *A&A* 350, 302–309, 1999.
- Usmanov, A.V. Interplanetary magnetic field structure and solar wind parameters as inferred from solar magnetic field observations and by using a numerical 2-D MHD model. *Solar Phys.* 143, 345–363, 1993a.
- Usmanov, A.V. A global numerical 3-D MHD model of the solar wind. *Solar Phys.* 146, 377–396, 1993b.
- Wang, A.-H., Wu, S.T., Suess, S.T., Poletto, G. A two-dimensional MHD global coronal model – Steady-state streamers. *Solar Phys.* 147, 55–71, 1993.
- Washimi, H., Ogino, T., Yoshino, Y. Two-dimensional structure of the solar wind near the sun. *Geo-phys. Res. Lett.* 14, 487–490, 1987.
- Wiegmann, T., Schindler, K., Neukirch, T. Helmet Streamers with Triple Structures: simulations of resistive dynamics. *Solar Phys.* 191, 391–407, 2000.
- Woo, R., Gazis, P.R. Mass flux in the ecliptic plane and near the Sun deduced from Doppler scintillation. *Geophys. Res. Lett.* 21, 1101–1104, 1994.